Preparation of Magadiite-Sodium Alginate Drug Carrier Composite by Pickering-Emulsion-Templated-Encapsulation Method and its Properties of Sustained Release Mechanism by Baker-Lonsdale and Korsmeyer-Peppas Model

Mingliang Ge
SCUT: South China University of Technology
Xinxiang Li
SCUT: South China University of Technology
Yueying Li
SCUT: South China University of Technology
Jahangir Alam S.M. (jahangirxmu@gmail.com)
SCUT: South China University of Technology
Yuee Gui
Guangzhou Women and Children's Medical Center
Yongchao Huang
SCUT: South China University of Technology
Luoxiang Cao
SCUT: South China University of Technology
Guodong Liang
Sun Yat-Sen University
Guoqing Hu
SCUT: South China University of Technology

Research Article

Keywords: Magadiite, Pickering emulsion, nanocomposite microspheres, drug carrier

Posted Date: November 11th, 2021

DOI: https://doi.org/10.21203/rs.3.rs-1066984/v1

Preparation of magadiite-sodium alginate drug carrier composite by Pickering-Emulsion-Templated-encapsulation method and its properties of sustained release mechanism by Baker-Lonsdale and Korsmeyer-Peppas model

Mingliang Ge [a, b, c], Xinxiang Li [a], Yueying Li [a], Jahangir Alam S.M. [a, *], Yuee Gui [d, *], Yongchao Huang [a], Luoxiang Cao [a], Guodong Liang [e], and Guoqing Hu [a]

[a] Key Laboratory of Polymer Processing Engineering of Ministry of Education, National Engineering Research Center of Novel Equipment for Polymer Processing, School of Mechanical & Automotive Engineering, South China University of Technology, Guangzhou 510640, China; gml@scut.edu.cn (M.G.); 201920101289@mail.scut.edu.cn, melyy_1996@mail.scut.edu.cn (Y.L.); mejahangir@scut.edu.cn (J.A.); guiyuee@sina.com (Y.G.); yongchaoHuang@163.com (Y.H.); luoxiangCao@163.com (L.C.); gqhu@scut.edu.cn (G.H.);

[c] Guizhou Minzu University, Guizhou 550025, China; gml@scut.edu.cn (M.G.);

[d] Guangzhou Women and Children's Medical Center, Guangzhou China; guiyuee@sina.com(Y.G.);

[b] Key Laboratory of Polymeric Composite & Functional Materials of Ministry of Education, Sun Yat-Sen University, Guangzhou 510275, China; lgdong@mail.sysu.edu.cn (G.L.);

* Correspondence: mejahangir@scut.edu.cn; Tel.: +86-132-502-54060, +86-135-339-19779

Abstract

In this study, the nanohybrid drug carrier were synthesized by Pickering emulsion-templated encapsulation (PETE) method to control the sustained-released properties of the nanohybrid drug carrier; magadiite-cetyltriphenyl phosphonium bromide (MAG-CTPB-KH550) and sodium alginate ($NaC_6H_7O_6$) was dissolved in the aqueous phase but metronidazole ($C_6H_9N_3O_3$) was dissolved in the ethyl acetate ($CH_3COOC_2H_5$) of the oil phase; both the oil phase and the aqueous phase were mixed and dispersed to prepared organically-modified magadiite-sodium alginate (MAG–CTPB–KH550/SA) nanohybrid drug carrier. X-ray diffraction (XRD), Flourier transform infrared spectrometry (FTIR) and scanning electron microscopy (SEM) results were shown that the most of Sodium alginate (SA) were encapsulated into the MAG–CTPB–KH550 but a few of SA were intercalated into the inner space layers of MAG–CTPB–KH550, metronidazole was combined with carrier materials through physical apparent adsorption, ion exchange and electrostatic interaction. In vitro result, it was showed that the slow release was shown less than 10% content of Sodium alginate; whereas, it was reduced the initial release rate of Metronidazole but it was extended the sustained-released time. To reach at equilibrium, the sustained-released effects of the drug carrier were prepared with 10% of Sodium Alginate for 32 h and the maximum cumulative release percentage was 93.42 for 24 h. First order model, Baker-Lonsdale model and Korsmeyer-Peppas model were fitted to study the slow-release mechanism; the correlation coefficients (R^2) of the three models were found over 0.9; thus, it was well described the release kinetics behavior of drug carrier composites. The slow-release mechanisms of the drug carrier were performed swelling and dissolving but the barrier effects of the lamina that were reduced the dissolution rate of metronidazole.

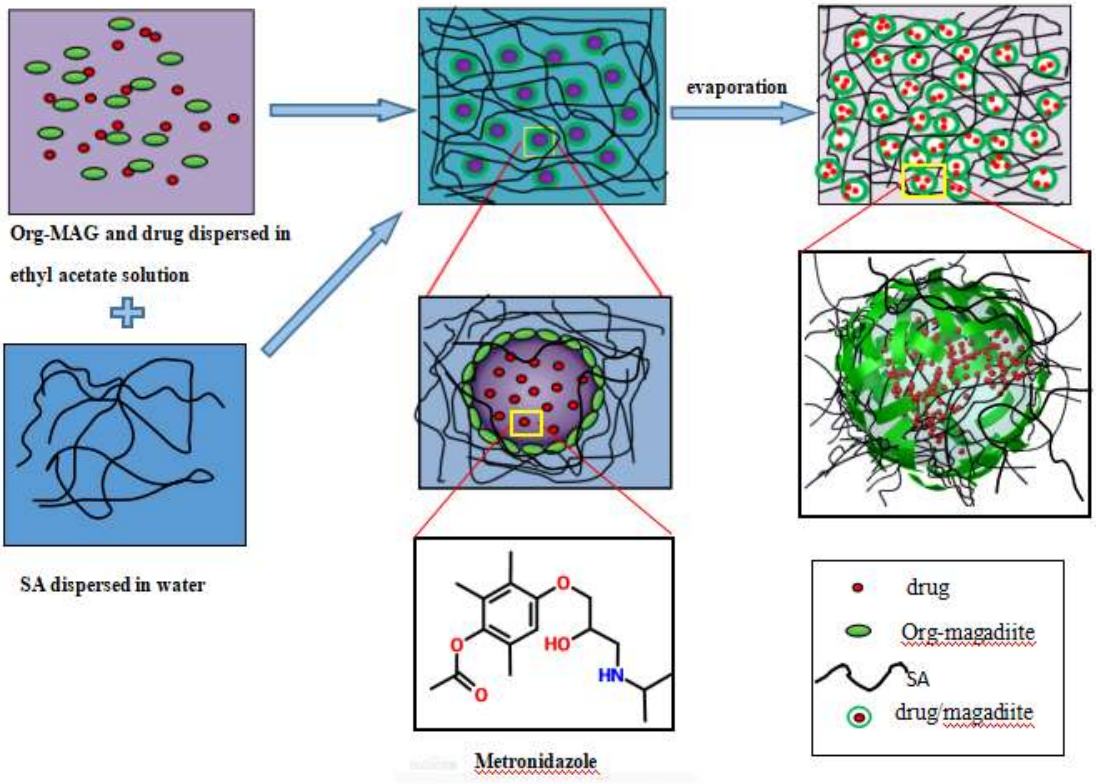

Keywords: Magadiite; Pickering emulsion; nanocomposite microspheres; drug carrier.

Introduction

Nowadays, controlled release drug carriers have attracted more and more researchers' because of their advantages, such as safety, low dosage, biocompatibility, and low toxic side effects via decreasing the drug release rate thereby, which have great practical significance for treating patients [1, 2]. Traditional drugs had burst release after administration, which lead to side effects and low efficiency-thus to solve these problems, many drug delivery and controlled release systems had been employed such as Liposomal drug delivery systems [3], Biocompatible PLGA Microspheres [4], Alginate/chitosan microparticles [5], three-dimensional poly (lactic-co-glycolic acid)/silica colloidal crystal drug delivery system [6], Mesoporous Silica Nanoparticles [7]. Metronidazole was used as antibacterial and antiprotozoal medication, generally arranged in the treatment of anti-anaerobic infections, follicle worms, and acne diseases, usually administered orally, and can be rapidly absorbed in gastric after administration [8,9]. Long-term and excessive using this drug leads to drug resistance and side effects, therefore, it is necessary to develop controlled release drug carriers to reduce the drug dose at an appropriate level. Sodium alginate has become a promising polysaccharide for drug carriers [10].

Alginate have been widely used as nanoparticles or microparticles for oral delivery of insulin [11-13], hemoglobin [14], probiotics [15,16], and cells [17] owing to its high biocompatibility and biodegradability [18]. The drug-loaded microspheres prepared by Sodium alginate alone have poor mechanical properties and drug loss during microsphere preparation, resulting in the uncontrollable release of the active pharmaceutical ingredient [19-21]. Many researchers had combined sodium alginate with other nanomaterials or polymers to modifying the structure of microspheres and improve the controlled release performance. Bardajee et al. [22] had prepared Thermo/pH/magnetic-triple sensitive nanogel comprised of SA and magnetic graphene oxide for anticancer drug delivery. Xie et al. [23] had prepared pH-sensitive Carboxymethyl chitosan sodium salt (CMCS)/ hydrogel drug carrier. SA was also used to prepare sustained drug release system with montmorillonite [24-26]. However, due to the low ion exchange capacity of montmorillonite, the prepared drug carrier was not ideal in sustained release time and drug loading performance. So a two-dimensional

layered silicate magadiite was developed in this study, which has special properties such as easily ion exchangeable hydrated sodium cations [27], active Si-OH groups on the layer, significant surface area associated with a negative charge, high ion exchange capacity (about 220 meq/100g) [28], excellent adsorption capacity and none toxic to the human body [29]. Magadiite used as drug carrier has been reported [29,30] and it can also be used as solid particle emulsifier in Pickering Emulsion-Templated Encapsulation.

Many methods were used in drug carrier preparation, such as solvent evaporation method [31], Spontaneous emulsification/solvent diffusion method [32], Biocompatible crosslinked polymer preparation method [33] and Pickering Emulsion-Templated Encapsulation method. Emulsion methods have the advantages of high encapsulation efficiency and superior storage stability [34]. But the application of emulsification-volatilization methods to prepare drug carriers has been limited because the emulsifier added must be a food-grade material and will not interfere with the performance of the drug. Pickering emulsion is made by amphiphilic solid particles which has a suitable particle size and surface wettability rather than organic surface-active agent. The mass fraction of active agents required for stable Pickering emulsion is obviously less than that of conventional emulsions, so Pickering emulsion was more environmentally friendly and cost saving [35-37]. Pickering Emulsion-Templated Encapsulation had been applied in the field of drug carrier [38-40].

In this study, an organic modified magadiite (magadiite (MAG), cetyltriphenyl phosphonium bromide (CTPB), and γ-aminopropyltriethoxysilane (KH550), SA, metronidazole (METZ) nano-hybrid drug carrier was prepared by the emulsification-volatilization method, the in vitro, stained release properties of Org-MAG/SA/metronidazole was studied by adjusting the content of magadiite and SA.

2. Experimental

2.1 Materials

Magadiite was prepared in the laboratory according to the referenced literature [41], Cetyltriphenyl phosphonium bromide was involved of analytical-grade reagent, which was

purchasedfrom Zhejiang Fenghong Clay Chemical Co., Ltd, China; Metronidazole was provided by Aladdin Ltd; SA and ethyl acetate were provided by Tianjin Fuchen Chemical Reagent Factory, China; Other chemicals of reagent grade were involved in all analytical-grade reagents that was purchased from Guangzhou Qianhui Company, China.

2.2 Preparation of hydrophobic organic-magadiite (Org-MAG)

Magadiite, Cetyltriphenyl phosphonium bromide and deionized water with a set mass ratio were mixed and magnetically stirred at 60℃ for 6 h, and then wash several times until the $AgNO_3$ test was negative. Separating the solid with filtration and dried at 80℃ for 12 h.

2.3 Preparation of Org-MAG/SA/metronidazole

30 mg metronidazole which was used as a simulated drug and a certain amount of Org-MAG were dispersed into 500 mL ethyl acetate solution as the oil phase, ultrasound treated for 10 minutes and then stirred. A certain amount of SA was dissolved in 500 mL of deionized water as the water phase. Finally, the ethyl acetate dispersion of Org-MAG and the sodium alginate solution were mixed and stirred for 1 h, formed a stable milky white Pickering emulsion. Thereafter, the ethyl acetate and the water were volatilized to obtained Org-MAG/SA/metronidazole drug carrier. The preparation process of drug carrier was shown in Fig. 1 and the content of SA and Org-MAG in different sample was shown in Table 1.

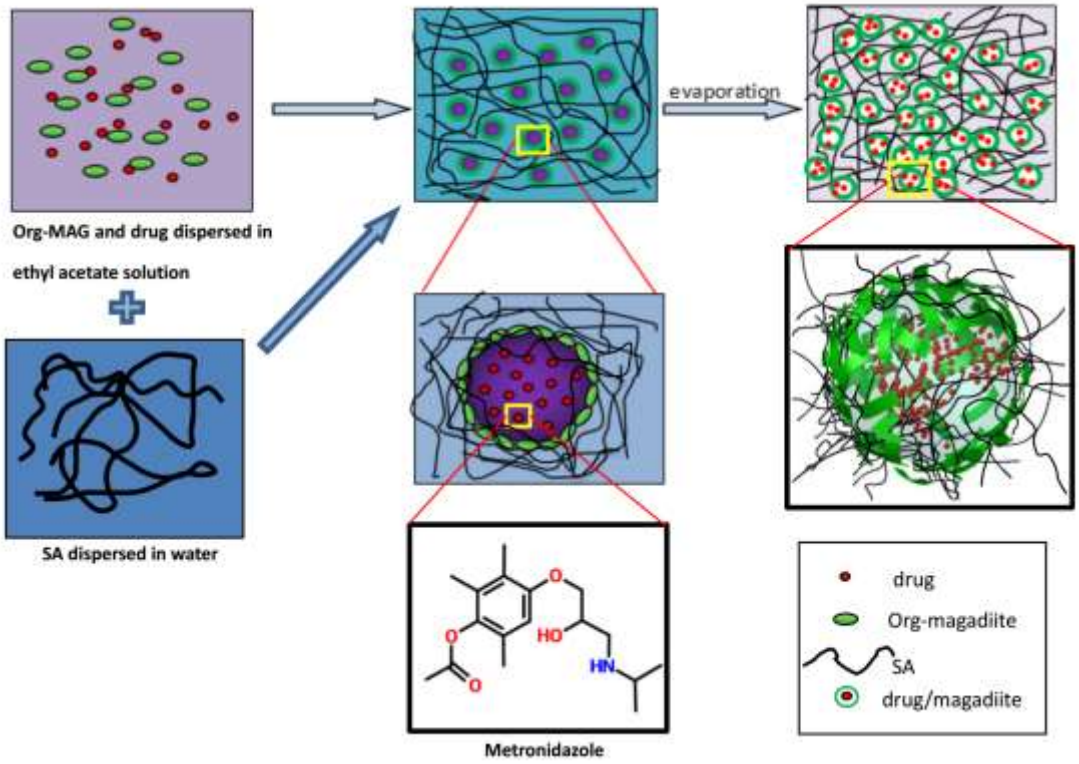

Fig. 1 preparation process of Org-MAG/SA drug carrier

Table 1. Content of SA and Org-MAG

Samples	S0	S1	S2	S3	S4	S5	S6
SA content (mg)	0	50	100	150	250	500	750
Org-MAG content(mg)	970	920	870	820	720	470	220

2.5 Metronidazole standard concentration curve drawing

UV/vis spectrophotometer was used to analyze the solution concentration and the optimum wavelength was 321 nm by wavelength scanning test. The concentration of metronidazole in solution was calculated by using the measured standard concentration curve. The linear equations of metronidazole in HCl solution of pH=4.0 were: $y=0.03387x+0.04483$, $R^2= 0.999$.

2.6 Characterization

2.6.1 X-ray powder diffraction

X-ray powder diffraction (Model D8 ADVANCE, Bruker AXS, Karlsruhe, Germany) patterns were recorded in the 2θ range of 2-10° at a scanning rate 6°/min and scanning step 0.02° using monochromatic Cu-Kα radiation with the tube voltage and the tube current was 40 KV and 40 mA.

2.6.2 Fourier transform infrared spectra

The spectral scanning rate of Fourier transform infrared spectra (NEXUS Model 670 Fourier, Thermo Nicolet Corporation, Waltham MA, USA) was 400~4000 cm^{-1}, the diameter of the sample was about 1 cm and the resolution ratio was 2 cm^{-1}.

2.6.3 Scanning electron microscopy

SEM analyses (Nova Nano SEM 430, FEI, Hillsboro, OR, USA) were used to observe the surface morphology of the drug carriers, the operating voltage was 10-20 kV.

2.7 Org-MAG/SA Drug carrier simulated sustained release in vitro

Metronidazole can be absorbed quickly and completely in gastric after oral administration and will be widely distributed in tissues and body fluids. In order to simulate the gastric juice environment, the drug carrier samples were subjected to in vitro simulated sustained release experiments under HCl solution of pH=4 at 37 °C. The amount of drug carrier loaded with metronidazole (1 g) was put into a pre-treated dialysis bag in a 100 mL slow-release medium and stirred. When the metronidazole drug was released for 0.5, 1, 2, 3, 4, 5, 6, 8, 10, 12, 24, 36 and 48 h, the amount of 5.0 mL upper clear liquid was taken out and concentration of metronidazole was tested using UV–vis spectrophotometer (at 321 nm). In order to maintain the consistency of the sustained release conditions, the amount of 5 mL release medium solution (at 37 °C) was poured back into the drug release system. The corresponding time concentration is calculated as follows:

$$C_n = X_n \quad (3\text{-}2)$$

The cumulative release amount for the corresponding time is calculated as follows:

$$Q_n = C_n V_0 + \sum_0^{n-1}(C_i V_e) \quad (3\text{-}3)$$

The cumulative release percentage of metronidazole in the corresponding time is calculated as follows

$$M = \frac{Q_n}{Q} \times 100\% \quad (3\text{-}4)$$

where n represents the number of times the buffer solution medium was taken out; C_n represents the cumulative release concentration of metronidazole when taking the buffer solution n times, mg/mL, and X_n represents the concentration of solution corresponding to the absorbance when taking the buffer solution n times, mg/mL; C_i represents the concentration of the replacement liquid taken at the i time, mg/mL; V_0 and V_e respectively represent the total volume of the initial sustained-release medium and the replacement volume of the sustained-release medium, mL; Q is drug loading capacity (mg/g) and Q_n is the cumulative release amount before the n-th replacement of buffer solution (mg/g); M represents the cumulative release percentage of metronidazole, %.

3. Results and discussion

3.1 Structural Characterization of Drug Carrier Composites

3.1.1 Scanning Electron Microscopy (SEM) analysis

The SEM images of the drug carriers with different content of SA were shown in Fig. 3. It can be seen from Fig. 3(a) that MAG has a layered structure with rosette morphology. Fig. 3(c) showed the microscopic morphology of S1, a portion of the metronidazole molecule can be observed as white small particles irregularly distributed between the layers of Org-MAG. Some of the SA molecule can only be observed on a few surfaces of Org-MAG layer as the content of SA was limited to 5%. As the content of SA increased (Fig. 3(d)), the boundary of the MAG interlayer became vague, while the surface morphology of the materials became flatter, a portion of metronidazole molecules were intercalated between the layers and another portion were attached to the surface in a block shape, which may be caused by random sorting of the MAG layers. When the content of SA was 25%, as shown in Fig. 3(e), blocks with different angularities can be observed, which was due to the SA attaching to the interlayer space of MAG, making the surface smooth, and a similar morphology was observed with SA content of 50% (Fig. 3(f)). In these two samples, metronidazole could not be observed on the surface of drug carrier, indicating that metronidazole was covered by SA. In Fig. 3(h)), the SA content was 75% and the surface of the drug carrier became flat. Because SA can form a film, which can wrap MAG more tightly, and when the content of SA increases to

a certain extent, SA was completely wrapped MAG, as is shown in Fig. 3 (S6).

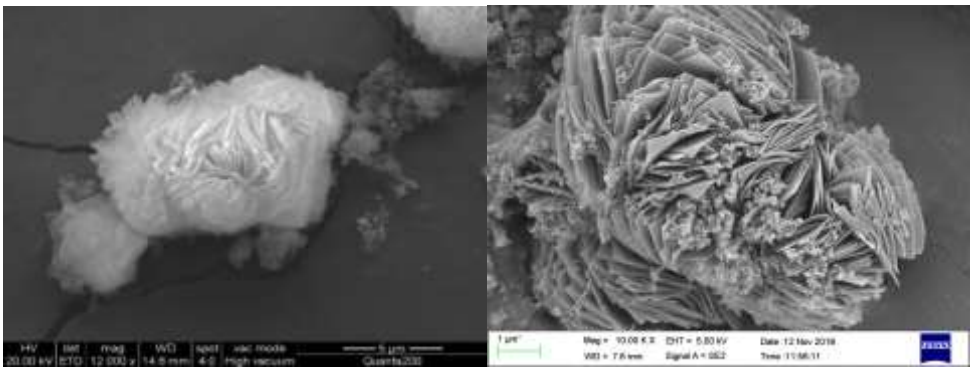

(a) MAG (b) S0

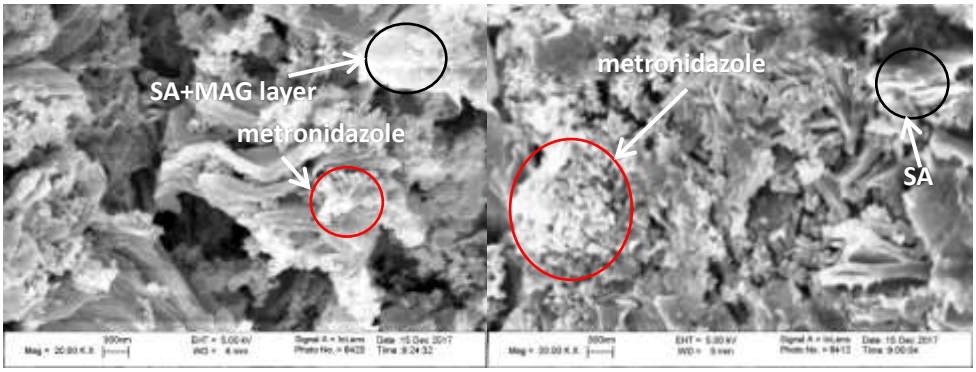

(c) S1 (d) S2

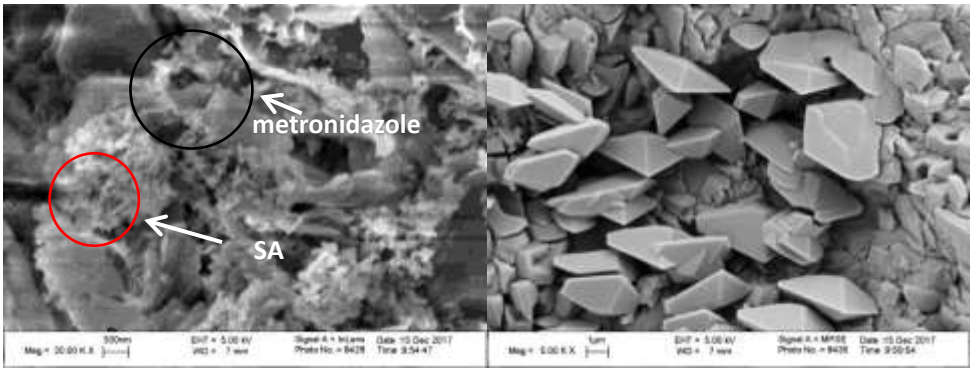

(e) S3 (f) S4

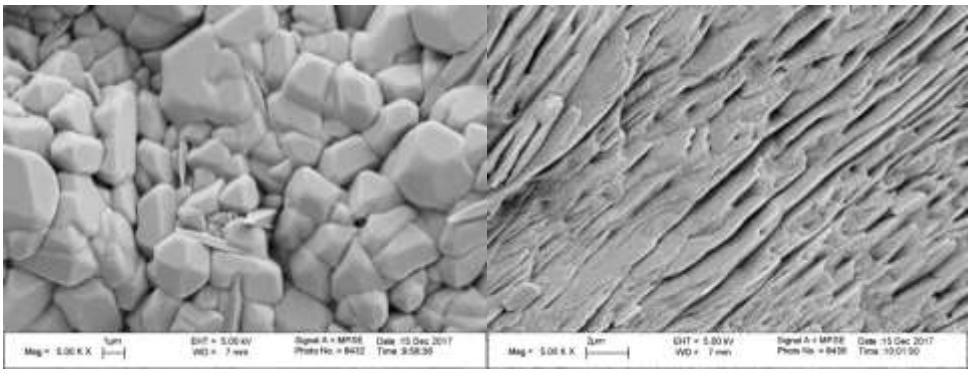

(g) S5 (h) S6

Fig. 3 SEM image of MAG(a) and Org-MAG/SA/metronidazole (b-h), the SA contents

were 0% (S0), 5% (S1), 10% (S2), 15% (S3), 25% (S4), 50% (S5), 75% (S6)

3.3.2 X-ray diffraction (XRD)

The XRD patterns of MAG, SA, Org-MAG, and Org-MAG/SA were shown in Figure 2. Comparing MAG (Fig. 2(a)) and Org-MAG (Fig. 2(b)) spectra, the XRD curve of MAG had an obvious 001 characteristic diffraction peak at 2θ=5.48°, and the corresponding layer spacing was 1.61 nm. After the modification of CTPB, the XRD patterns of Org-MAG changed significantly: 001 characteristic diffraction peak moved to 2θ=2.65°, and the corresponding layer spacing increased to 3.33 nm. The original diffraction peak at 2θ=5.48° basically disappeared, while a weak diffraction peak appeared at 2θ=4.62°, in which the layer spacing was 1.91nm, almost identical to that of pure MAG. From the results above, it could be referred that part of the organic modifier could intercalate into the layers of MAG, expending the interlayer structure space. The XRD diagram of Org-MAG/SA was shown in Fig. 2(c); it can be seen that the characteristic diffraction peak at 2θ=2.65° on Org-MAG (Fig. 2(b)) didn't change, but the intensity increased significantly, and the peak at 2θ=4.62° on Org-MAG (Fig. 2(c)) transferred to 2θ=5.40°, the interlayer space of Org-MAG/SA was roughly same to Org-MAG. From Fig. 2(d), it could be seen that there was no characteristic diffraction peak in the measurement range of SA. The result indicated that the addition of SA didn't change the structure of Org-MAG. Although the ordered structure was destroyed to a certain extent, its overall crystal and layered structure were not destroyed. This is consistent with the phenomenon observed in SEM images

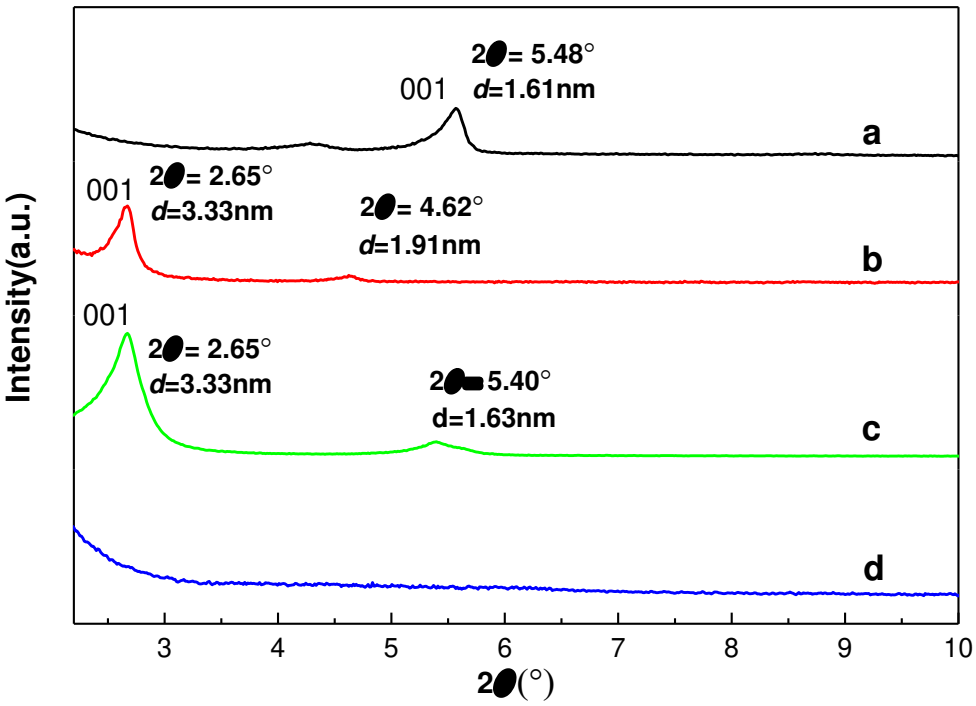

Fig. 2 XRD pattern of (a) MAG, (b) Org-MAG, (c) Org-MAG/SA, (d) SA

3.1.3 Fourier transform infrared spectroscopy (FTIR)

Fig. 4 exhibits the chemical structure of Org-MAG, SA, and Org-MAG/SA/metronidazole which refers to the FTIR spectrum. In Fig. 4(b) the absorption peaks at 3451 cm^{-1}, 1643 cm^{-1}, 1420 cm^{-1}, 1322 cm^{-1}, and 1137 cm^{-1} were assigned to the stretching vibration of -OH, C=C, C=OH, C-O-C and C-O, respectively [42]. Fig. 4(d) was the FTIR spectrum of Org-MAG/SA/metronidazole. Compared with the FTIR spectra of Org-MAG showed in Fig. 4(c), it was found that the characteristic absorption peaks at 2923 cm^{-1} and 2861 cm^{-1} caused by organic modifiers intercalated into the MAG interlayer disappeared, which indicated that due to the preparation of drug carrier, the characteristic absorption peaks at 2923 cm^{-1} and 2861 cm^{-1} had disappeared. The organic modifier was exfoliated from the interlayer of MAG, while metronidazole entered the MAG interlayer and was coated by the MAG interlayer, which was corresponding to XRD pattern mentioned above [43]. Compared with the standard FTIR spectra of metronidazole, the characteristic absorption peak between the wave number of 1500-400 cm^{-1} has a large multi-peak superposition, which also indicated that

metronidazole was encapsulated inside the Org-MAG/SA/metronidazole [44]. The expansion vibration absorption peak of the C-N single bond was between the wave number of 1300-900 cm^{-1}, the absorption peak intensity of the C-N group was reduced since the oxygen atom in the molecule of metronidazole and was close to the -C-N group; thus, that the intensity of the absorption peak of the C-N group was small. Therefore, several stretching vibration absorption peaks of C-N bond at the wave number of 1300-900 cm^{-1} will be combined into a single absorption peak with very small intensity and large width.

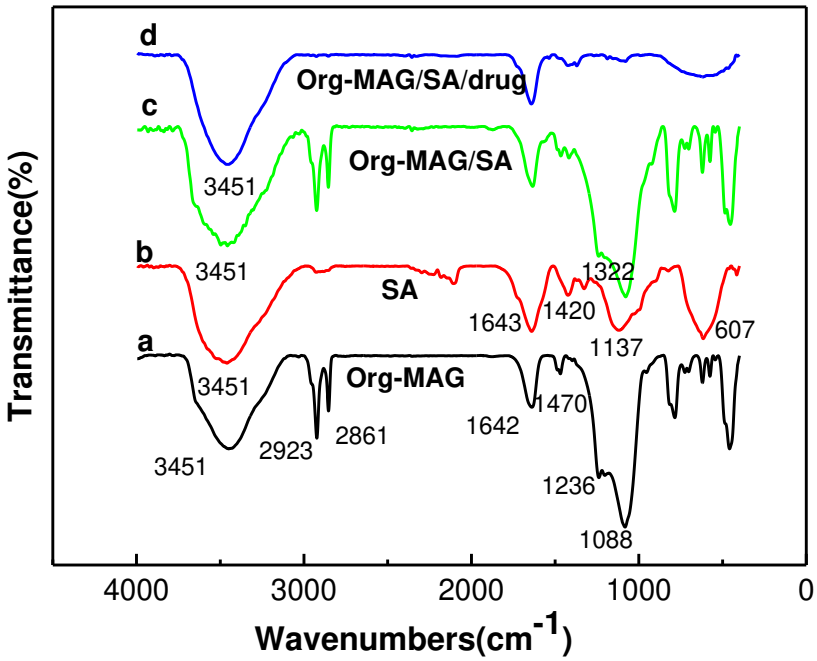

Fig. 4 Infrared spectrum of (a) MAG, (b) SA, (c) Org-MAG, (d) Org-MAG/SA/metronidazole (S2)

3.2 Sodium alginate/magadiite drug release in vitro

The cumulative release rates for different content of SA were shown in Fig. 5 and the maximum cumulative release amount and cumulative release percentage were shown in Table 2, which showed that the final release rate of Org-MAG was very low, indicating that most of the drugs hadn't released. The main reason was the adsorption effect of MAG layers [45]. When a certain amount of SA was added, the cumulative release rate was increasing continuously until the content of SA was 10%, reaching the maximum value of 93.42%. It can be seen that the addition of SA can significantly increase the release amount of the drug, the

low release rate of Org-MAG was due to the fact that the drug in the Org-MAG interlayer was obstructed and adsorbed by the layer so that it cannot be released. Meanwhile the addition of SA expands the interlayer spacing of MAG, a good agreement with the XRD results of Fig. 2, reduces the interaction between drug molecules and MAG layer. When the content of SA was excessive, as shown by electron microscope (Fig. 3 (g, h)), the layer space of MAG was completely encapsulated by SA, which leads to the impossibility of releasing the drugs in MAG layer.

Table 3 showed time acquired for the release rate reach to 90% of the balance release rate, and it can be seen that with the increasing of SA content, the drug release rate had slowed down (the time of S1, S2 and S3 were over 20 h), and when the SA content was 10%, the release took the longest time to reach balance. As the SA content continuously increased, the time acquired to reach 90% of the drug balance release rate became shorter. The reason was that appropriate amount of SA can encapsulate a part of the drug, when the drug released in-vitro, the drug at the edge of the MAG layer released first, but the drug between the layers cannot released immediately due to the blocking effect of SA macromolecules and MAG layer, resulting in low drug release rate and effectively slow release. When SA was further increased, the layer space of MAG was completely encapsulated by SA, as shown by electron microscopy (in Fig. 3), so during the in-vitro release, only drugs adsorbed outside the MAG layer can be released in an even faster rate, but the drug between the MAG layers coated by SA was difficult to release, because SA was difficult to dissolve in acid solution.

In general, the release of a biodegradable polymer-loaded drug in vitro was controlled by three mechanisms: diffusion of drug molecules, biodegradation of high molecular polymers, and swelling or dissolution of high molecular polymers [46]. The sustained release steps of drug carriers could be generally divided into two stages: first, the drug attached to the surface of the drug carrier diffuses in the buffer medium, and secondly, the polymer swells and dissolves in the solution. The sustained release figure reveals that the release rate of different drug carriers was fast within 0~4 h and slow down after 4 h.

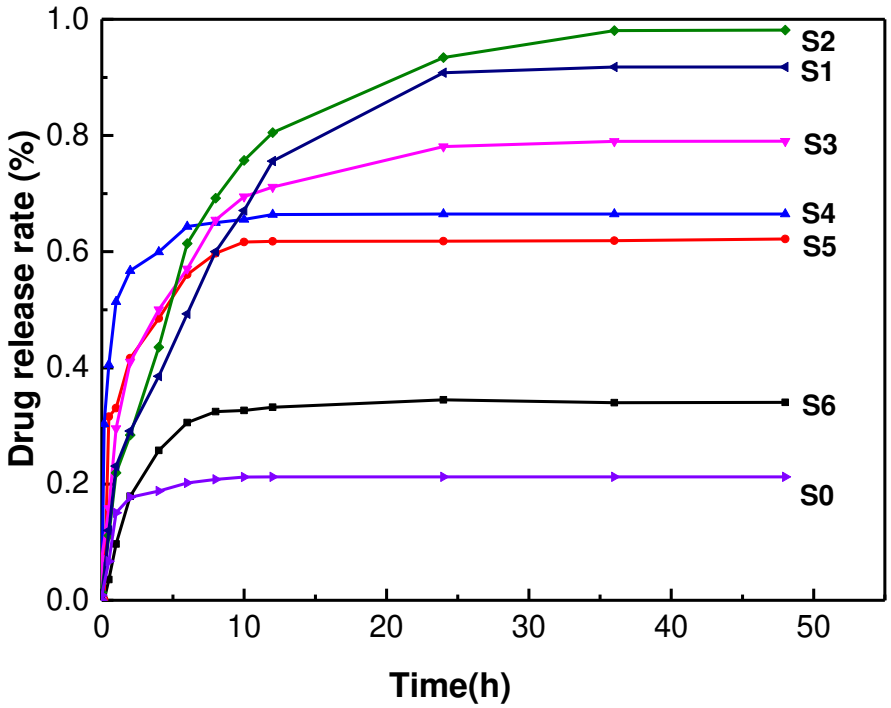

Fig. 5 The balance release rate of different content of SA

(S0) Org-MAG, (S1)5%, (S2) 10%, (S3) 15%, (S4) 25%, (S5)50%, (S6) 75%

Table 2 Maximum cumulative release and cumulative release percentage after 24 hours of release

Samples	S0	S1	S2	S3	S4	S5	S6
Drug release rate / (%)	21.23	90.8	93.42	78.08	47.48	35.39	34.50

Table 3 Time for the release rate reach to 90% of balance release rate

Samples	S0	S1	S2	S3	S4	S5	S6
Time to reach 90% of the balance release rate / h	8	21	32	23	6	5.5	5

3.3 Drug release kinetics study

The study of drug release kinetics is helpful to understand the mechanism of drug release.

The analysis of the drug delivery process of Org-MAG/SA drug carrier in vitro shows that the sustained release of Pickering emulsion drug carrier consists of diffusion in buffer medium, swelling and dissolution of the polymer, and interlayer diffusion. The drug molecules encapsulated by drug carriers may diffuse into the release medium through the swelling and dissolution of polymers, and the small interaction between drug molecules and layered lamellae and polymers will affect the release kinetics. Under the example of the sustained release of drug carrier (S2), the kinetics fitting analysis of the sustained release process was carried out.

The sustained release of metronidazole of the drug carrier may undergo several steps, one is the diffusion of the drug in the interlayer; the second is the solid-liquid boundary of the drug between the MAG and the release medium, in which liquid film diffusion occurs, and the third stage is the concentration gradient diffusion of the drug in the release medium. The release behavior was studied using the Zero order model, the First order model, the Higuchi model, the release-time reciprocal model, the Baker-Lonsdale model, and the Korsmeyer-Peppas model [45,46].

Zero-order model expression:

$$Q_t = k_0 t + C_0 \quad (1)$$

First order model expression:

$$-\ln\left(1 - \frac{Q_t}{Q_\infty}\right) = k_1 t + C_1 \quad (2)$$

Baker-Lonsdale model expression:

$$\frac{3}{2}\left[1 - \left(1 - \frac{Q_t}{Q_\infty}\right)^{\frac{2}{3}}\right] - \frac{Q_t}{Q_\infty} = k_2 t \quad (3)$$

Korsmeyer-Peppas model expression:

$$ln\frac{Q_t}{Q_\infty} = nlnt + C_{KP} \quad (4)$$

In the above expressions, Q_t and Q_∞ represent the cumulative release amount and maximum cumulative release of metronidazole during t time respectively, mg/g; k_0, k_1, k_2, and n represent the release constants in the corresponding kinetic model, respectively; For release time, h; C_0, C_1, and C_{KP} represent the constants in the corresponding kinetic model, respectively.

The relevant parameters for a linear fitting of the release kinetic model of S2 are shown in

Table 3. It can be seen from the data that the linear correlation coefficients of the first order model, Baker-Lonsdale and Korsmeyer-Peppas models for drug sustained-release fitting are above 0.9. All three models can describe the sustained release process of drug carrier. Among the four models, First-order model has the highest linear correlation coefficient, indicating it is the best one to describe the release kinetic behavior of the composite drug carrier, while the zero-order model does not match.

Fig. 6 showed the fitting curves of different models for drug composite carriers and the fitting parameters of S2 under different release kinetic models were showed in Table 4. In the Korsmeyer-Peppas model, n is the diffusion index, and its value can be used to describe the drug release mechanism. The value of n is between 0.43 and 0.85, indicating that the sustained release mechanism of the composite carrier to metronidazole belongs to non-Fick diffusion, which is the synergistic effect of drug diffusion and matrix dissolution, which may be due to the barrier effect of the interlayer space of MAG and the swelling and dissolution of SA [47]. The release kinetics of the drug carrier also fits well with the First-order model, indicating that the sustained release of metronidazole is related to its concentration profile in the laminate structure of the carrier material [48-50], mainly due to the presence of layers in the MAG. The drug molecule is limited by the MAG interlayer space and the encapsulation of SA, and the MAG interlayer space has an inhibitory effect on the in vitro dissolution of metronidazole, thus causing a change in release rate.

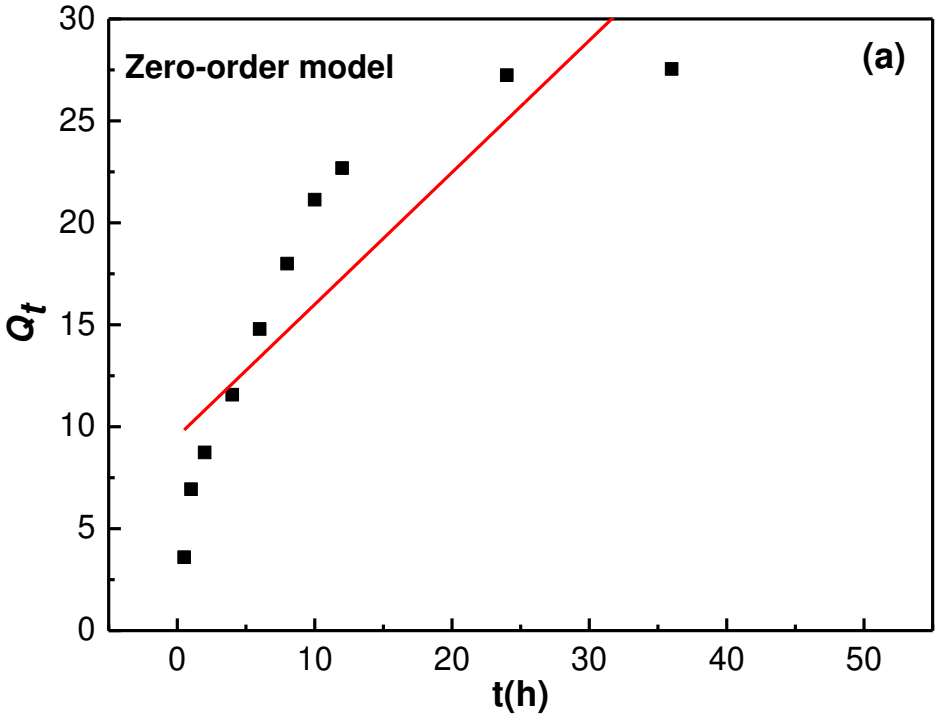
Zero-order model
(a)
Q_t
t(h)
0
5
10
15
20
25
30
0
10
20
30
40
50

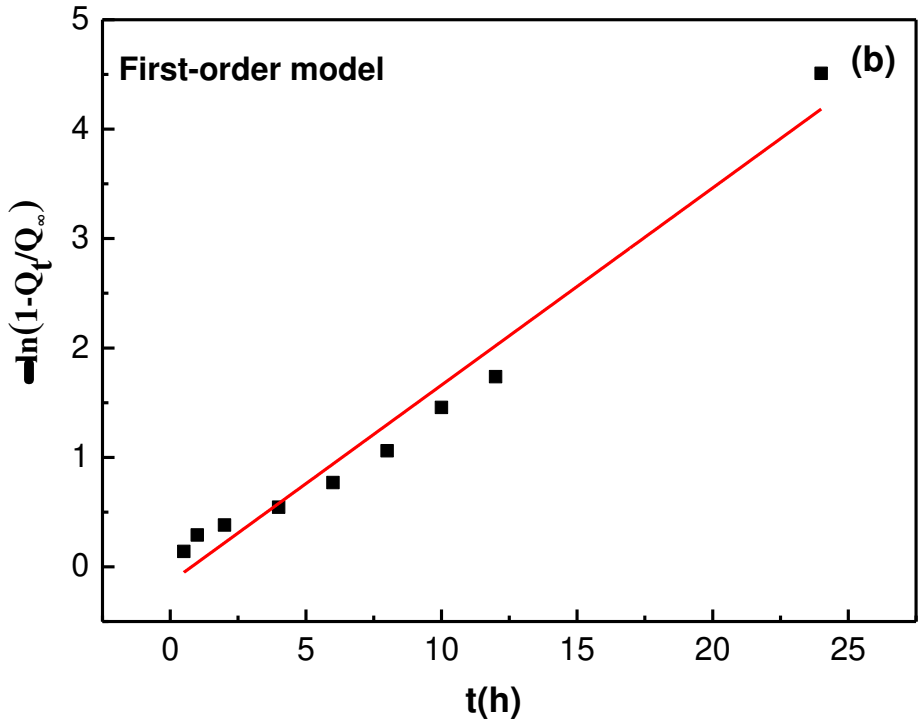
First-order model
(b)
$-\ln(1-Q_t/Q_\infty)$
t(h)
0
1
2
3
4
5
0
5
10
15
20
25

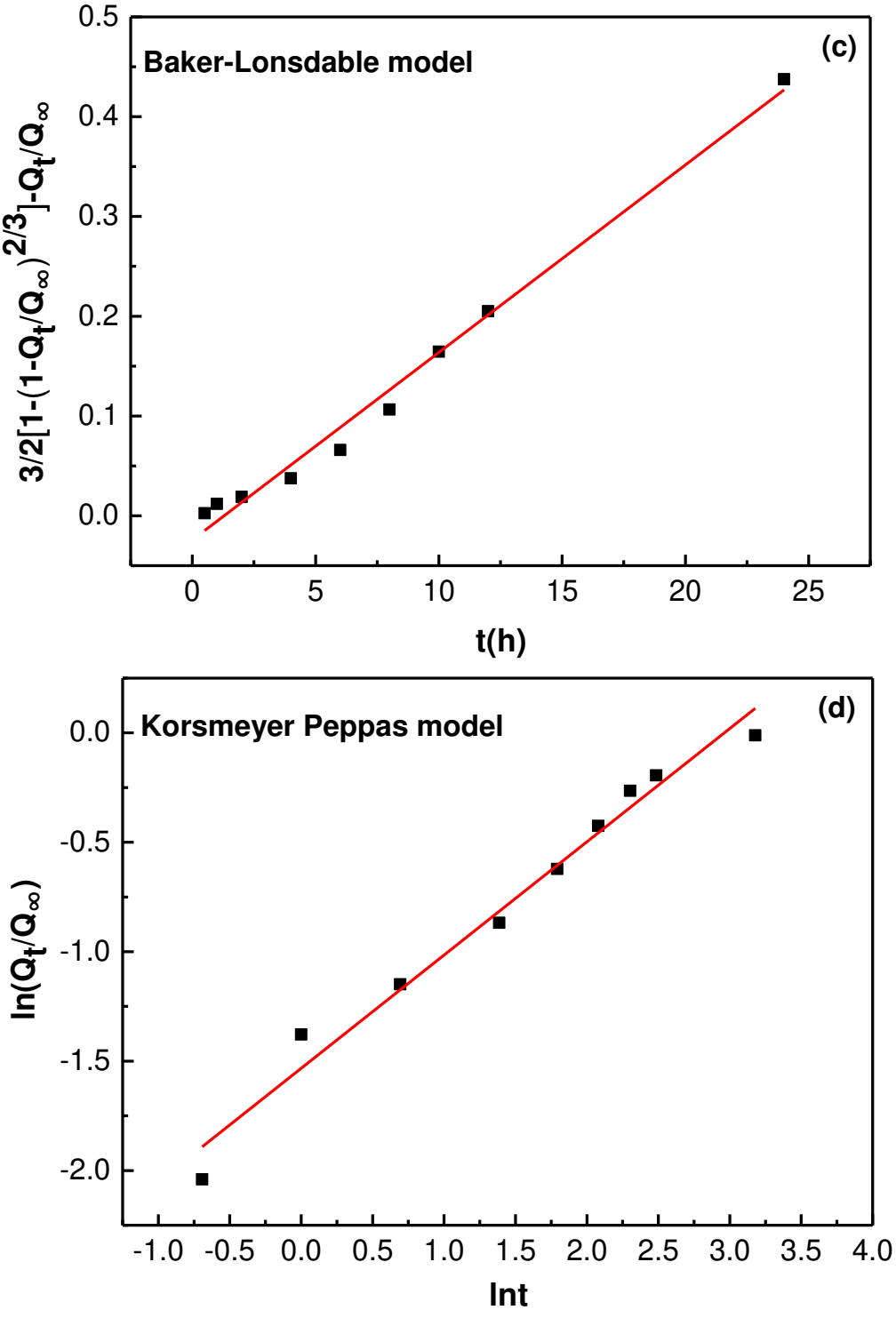

Fig. 6 The fitting curves of different models

Table 4 Fitting parameters of S2 under different release kinetic models

Sample	Zero-order equation		First-order equation		Baker-Lonsdable equation		Korsmeyer-Peppas model	
	K_0	R^2	K_1	R^2	K_2	R^2	n	R^2

S2	0.7680	0.673	0.1999	0.975	0.0153	0.942	0.6578	0.911

4. Conclusions

In this study, a serious of Org-MAG/SA drug carriers containing metronidazole were prepared through Pickering Emulsion-Templated Encapsulation and their controllable sustained release property were studied. XRD, FT-IR, and SEM analysis showed that the majority of SA encapsulated the Org-MAG, and a few SA was intercalated into the Org-MAG inner space layers. Metronidazole was combined with the carrier material through physical apparent adsorption, electrostatic action, and coating mechanism.

In vitro release test was conducted in the condition that the pH was determined to be 4 to simulate gastric the acid-base environment in which the metronidazole was released after oral administration. SA content has a significant influence on the sustained release of metronidazole, a small amount of SA (5% - 10%) can braced layer the Org-MAG inner layer and formed a film to wrap the lamellar spacing, which can prevent metronidazole from completely stuck in the drug carrier, this helped to increase drug release amount and slow down release rate. But if the SA was excess (more than 15%), the loaded drug cannot go through the thick SA film and release. The Pickering drug carrier prepared by 10% SA reached a balance in over 32h. Metronidazole which encapsulated by MAG and SA in drug carrier can maintained a relatively low release rate because of the drug carrier's mesoporous structures, the swelling and dissolution of SA and the barrier effect of the MAG layer.

Ethics approval and consent to participate: Not Applicable.

Consent for publication: All the authors are agreed for publication.

Availability of data and materials: Not Applicable.

Competing interests: Not Applicable.

Conflicts of Interest: The authors declare no conflict of interest. The funders had no role in the design of the study; in the collection, analyses, or interpretation of data; in the writing of the manuscript, and in the decision to publish the results.

Funding: The authors gratefully acknowledge the financial support of this research work by Natural Science Foundation of Guangdong Province Project (Project No. 2016A030313520), Key Laboratory of Polymeric Composite & Functional Materials of Ministry of Education Project (Project No. PCFM-2017–02), Guangdong Water Conservancy Science and Technology Innovation Project (Project No. 2017–24), Science and Technology Program of Guangzhou in China (Project No. 202102080477), and Guangdong Provincial Department of Education Featured Innovation Project (Project No. 2017KTSCX007).

Authors' Contributions: Conceptualization, Mingliang Ge, Yuee Gui and Guodong Liang; Data curation, Jahangir Alam S.M., Yongchao Huang, Luoxiang Cao and Guodong Liang; Formal analysis, Jahangir Alam S.M. and Yongchao Huang; Funding acquisition, Mingliang Ge; Investigation, Mingliang Ge, Yueying Li and Yuee Gui; Methodology, Mingliang Ge, Yueying Li , Jahangir Alam S.M., Yuee Gui, Yongchao Huang, Luoxiang Cao and Guodong Liang; Project administration, Mingliang Ge and Guoqing Hu; Resources, Mingliang Ge, Yuee Gui, Guodong Liang and Guoqing Hu; Software, Jahangir Alam S.M. and Yongchao Huang; Supervision, Mingliang Ge; Validation, Mingliang Ge, Yueying Li , Yuee Gui, Luoxiang Cao and Guodong Liang; Visualization, Yueying Li , Jahangir Alam S.M., Luoxiang Cao; Writing – original draft, Yueying Li ; Writing – review & editing, Jahangir Alam S.M., and Guoqing Hu.

Acknowledgments: The authors gratefully acknowledge the financial support of this research work by the Natural Science Foundation of Guangdong Province Project (Project No. 2016A030313520), Key Laboratory of Polymeric Composite & Functional Materials of Ministry of Education Project (Project No. PCFM-2017-02), Guangdong Water Conservancy Science and Technology Innovation Project (Project No. 2017-24), Science and Technology Program of Guangzhou in China (Project No. 202102080477), and Guangdong Provincial Department of Education Featured Innovation Project (Project No. 2017KTSCX007). The authors gratefully thank the reviewers for their valuable review comments to enrich the publication.

References

[1] Yang J, Chen J, Pan D, Wan Y, Wang Z. pH-sensitive interpenetrating network hydrogels based on chitosan derivatives and alginate for oral drug delivery. *Carbohydrate Polymers* **2013**, *92, 719-725.*

[2] Eugster H.P. Hydrous sodium silicate from Lake Magadi, Kenya, precursors of bedded chert. *Science* **1967**, *157,* 1177-1179.

[3] Allen TM, Cullis PR. Liposomal drug delivery systems: From concept to clinical applications. *Advanced Drug Delivery Reviews* **2013**, *65*,36–48.

[4] Pal K, Laha D, Parida PK, Roy S, Bardhan S, Dutta A, et al. An In Vivo Study for Targeted Delivery of Curcumin in Human Triple Negative Breast Carcinoma Cells Using Biocompatible PLGA Microspheres Conjugated with Folic Acid. *Journal of Nanoscience and Nanotechnology* **2019**, *19*, 3720-3733.

[5] Ling K, Wu H, Neish AS, Champion JA. Alginate/chitosan microparticles for gastric passage and intestinal release of therapeutic protein nanoparticles. *Journal of Controlled Release* **2019**, *295*,174–186.

[6] Guo R, Sun X-T, Zhang Y, Wang D-N, Yang C-G, Xu Z-R. Three-dimensional poly(lactic-co-glycolic acid)/silica colloidal crystal microparticles for sustained drug release and visualized monitoring. *J Colloid Interface Sc* **2018**, *530*,465–472.

[7] Porgham D, Dusti T, Hossein K, Akbarijavar H, Khoobi M, Seyedjafari E, Birhanu G, Khosravian P, SadatMahdavi F. Poly-l-lactic acid scaffold incorporated chitosan-coated mesoporous silica nanoparticles as pH-sensitive composite for enhanced osteogenic differentiation of human adipose tissue stem cells by dexamethasone delivery. *Artificial cells, nanomedicine, and biotechnology* **2019**, *47*, 4020-4029.

[8] Tang F, Li L, Chen D. Mesoporous Silica Nanoparticles: Synthesis, Biocompatibility and Drug Delivery. *Advanced Materials* **2012**, *24*,1504–1534.

[9] Mehrzad-Samarin M, Faridbod F, Dezfuli AS, Ganjali MR. A novel metronidazole fluorescent nanosensor based on graphene quantum dots embedded silica molecularly imprinted polymer. *Biosens Bioelectron* **2017**, *92*, 618–623.

[10] Pawar SN, Edgar KJ. Alginate derivatization: A review of chemistry, properties and applications. *Biomaterials 2012*, *33*, 3279–3305.

[11] Zhang Y, Wei W, Lv P, Wang L, Ma G. Preparation and evaluation of alginate–chitosan microspheres for oral delivery of insulin. *European Journal of Pharmaceutics and Biopharmaceutics* **2011**, *77*, 11–19.

[12] Sarmento B, Ribeiro A, Veiga F, Sampaio P, Neufeld R, Ferreira D. Alginate/Chitosan Nanoparticles are Effective for Oral Insulin Delivery. *Pharmaceutical Research* **2007**, *24*, 2198–2206.

[13] Mukhopadhyay P, Chakraborty S, Bhattacharya S, Mishra R, Kundu PP. pH-sensitive chitosan/alginate core-shell nanoparticles for efficient and safe oral insulin delivery. *International Journal of Biological Macromolecules* **2015**, *72*, 640–648.

[14] Ribeiro AJ, Silva C, Ferreira D, Veiga F. Chitosan-reinforced alginate microspheres obtained

through the emulsification/internal gelation technique. *European Journal of Pharmaceutical Sciences* **2005**, *25*, 31–40.
[15] Chávarri M, Marañón I, Ares R, Ibáñez FC, Marzo F, Villarán M del C. Microencapsulation of a probiotic and prebiotic in alginate-chitosan capsules improves survival in simulated gastro-intestinal conditions. *International Journal of Food Microbiology* **2010**, *142*, 185–189.
[16] Cook MT, Tzortzis G, Charalampopoulos D, Khutoryanskiy VV. Production and Evaluation of Dry Alginate-Chitosan Microcapsules as an Enteric Delivery Vehicle for Probiotic Bacteria. *Biomacromolecules* **2011**, *12*, 2834–2840.
[17] Tan W-H, Takeuchi S. Monodisperse Alginate Hydrogel Microbeads for Cell Encapsulation. *Advanced Materials* **2007**, *19*, 2696–2701.
[18] Tsirigotis-Maniecka M, Gancarz R, Wilk KA. Preparation and characterization of sodium alginate/chitosan microparticles containing esculin. *Colloids and Surfaces A-physicochemical and Engineering Aspects* ***2016***, *510*, 22-32.
[19] Liu P, Krishnan TR. Alginate-Pectin-Poly-L-lysine Particulate as a Potential Controlled Release Formulation. *Journal of Pharmacy and Pharmacology* **1999**, *51*, 141–9.
[20] Kulkarni AR, Soppimath KS, Aralaguppi MI, Aminabhavi TM, Rudzinski WE. Preparation of Cross-Linked Sodium Alginate Microparticles Using Glutaraldehyde in Methanol. *Drug Development and Industrial Pharmacy* **2000**, *26*, 1121–1124.
[21] Kulkarni AR, Soppimath KS, Aminabhavi TM, Dave AM, Mehta MH. Glutaraldehyde crosslinked sodium alginate beads containing liquid pesticide for soil application. *Journal of Controlled Release* **2000**, *63*, 97–105.
[22] Bardajee GR, Hooshyar Z. Thermo/pH/magnetic-triple sensitive poly(N-isopropylacrylamide-co-2-dimethylaminoethyl) methacrylate)/sodium alginate modified magnetic graphene oxide nanogel for anticancer drug delivery. *Polym Bull* **2018**, *75*, 5403–5419.
[23] Xie C-X, Tian T-C, Yu S-T, Li L. pH-sensitive hydrogel based on carboxymethyl chitosan/sodium alginate and its application for drug delivery. *Journal of Applied Polymer Science* **2019**, *136*, 46911.
[24] Yan H, Chen X, Feng Y, Xiang F, Li J, Shi Z, et al. Modification of montmorillonite by ball-milling method for immobilization and delivery of acetamiprid based on alginate/exfoliated montmorillonite nanocomposite. *Polym Bull* **2016**, *73*, 1185–1206.
[25] Iliescu RI, Andronescu E, Ghitulica CD, Voicu G, Ficai A, Hoteteu M. Montmorillonite–alginate nanocomposite as a drug delivery system – incorporation and in vitro release of irinotecan. *International Journal of Pharmaceutics* **2014**, *463*, 184–192.
[26] Mokhtar A, Djelad A, Adjdir M, Zahraoui M, Bengueddach A, Sassi M. Intercalation of hydrophilic antibiotic into the interlayer space of the layered silicate magadiite. *Journal of Molecular Structure* **2018**, *1171*, 190–195.
[27] Homhuan N, Bureekaew S, Ogawa M. Efficient Concentration of Indium(III) from Aqueous Solution Using Layered Silicates. *Langmuir* **2017**, *33*, 9558–9564.
[28] S.M. Auerbach, K.A. Carrado, P.K. Dutta, Handbook of Layered Materials, CRC Press, 2004.
[29] Ge M, Cao L, Du M, Hu G, Jahangir Alam SM. Competitive adsorption analyses of a pure magadiite and a new silylated magadiite on methylene blue and phenol from related aqueous solution. *Materials Chemistry and Physics* **2018**, *217*, 393–402.
[30] Ge M, Wang X, Du M, Liang G, Hu G, S. M. JA. Adsorption Analyses of Phenol from Aqueous Solutions Using Magadiite Modified with Organo-Functional Groups: Kinetic and Equilibrium Studies. *Materials* **2019**, *12*, 96.
[31] Pathak C P, Sawhney A S, Edelman P G, Chandrashekhar, Bennett S. Biocompatible crosslinked polymer preparation by nucleophilic-electrophilic group reaction between functional polymer and crosslinking agent, useful e.g. for preventing surgical adhesions or for drug delivery: WO 200033764-A1[P]. *2000 -6-15*.
[32] Soppimath KS, Aminabhavi TM, Kulkarni AR, Rudzinski WE. Biodegradable polymeric nanoparticles as drug delivery devices. *Journal of Controlled Release* **2001**, *70*, 1–20.
[33] Khodaverdi E, Tayarani-Najaran Z, Minbashi E, Alibolandi M, Hosseini J, Sepahi S, et al. Docetaxel-Loaded Mixed Micelles and Polymersomes Composed of Poly (caprolactone)-Poly (ethylene glycol) (PEG-PCL) and Poly (lactic acid)-Poly (ethylene glycol) (PEG-PLA): Preparation and In-vitro Characterization. *Iran J Pharm Res* **2019**, *18*, 142–55.
[34] Aveyard R, Binks BP, Clint JH. Emulsions stabilised solely by colloidal particles. *Advances in Colloid and Interface Science*. 2003, *100–102:503–46*.
[35] Low LE, Tan LT-H, Goh B-H, Tey BT, Ong BH, Tang SY. Magnetic cellulose nanocrystal stabilized

Pickering emulsions for enhanced bioactive release and human colon cancer therapy. *International Journal of Biological Macromolecules* **2019**, *127*, 76–84.
[36] Wang X, Yu K, An R, Han L, Zhang Y, Shi L, et al. Self-assembling GO/modified HEC hybrid stabilized pickering emulsions and template polymerization for biomedical hydrogels. *Carbohydrate Polymers* **2019**, *207*, 694–703.
[37] Javanbakht S, Shaabani A. Encapsulation of graphene quantum dot-crosslinked chitosan by carboxymethylcellulose hydrogel beads as a pH-responsive bio-nanocomposite for the oral delivery agent. *International Journal of Biological Macromolecules* **2019**, *123*, 389–397.
[38] Goenka S, Sant V, Sant S. Graphene-based nanomaterials for drug delivery and tissue engineering. *Journal of Controlled Release* **2014**, *173*, 75–88.
[39] Marku D, Wahlgren M, Rayner M, Sjöö M, Timgren A. Characterization of starch Pickering emulsions for potential applications in topical formulations. *International Journal of Pharmaceutics* **2012**, *428*, 1–7.
[40] Akhavan O, Ghaderi E, Aghayee S, Fereydooni Y, Talebi A. The use of a glucose-reduced graphene oxide suspension for photothermal cancer therapy. *Journal of Materials Chemistry* **2012**, *22*, 13773–13781.
[41] Ge M, Xi Z, Zhu C, Liang G, Hu G, Jamal L, et al. Preparation and Characterization of Magadiite–Magnetite Nanocomposite with Its Sorption Performance Analyses on Removal of Methylene Blue from Aqueous Solutions. *Polymers* **2019**, *11*, 607.
[42] Yin G, Zheng Z, Wang H, Du Q. Slightly surface-functionalized polystyrene microspheres prepared via Pickering emulsion polymerization using for electrophoretic displays. *Journal of Colloid and Interface Science* **2011**, *361*, 456–464.
[43] Ge, M.; Cao, L.; Du, M.; Hu, G.; Jahangir Alam, S.M. Adsorptive characterization of a pure magadiite and an organic modified magadiite on removal of methylene blue from related aqueous solution. Mater. Chem. and Phys. 2018; 217, 533–40.Barthelat F. Nacre from mollusk shells: a model for high-performance structural materials. *Bioinspir Biomim* **2010**, *5*, 035001.
[44] Tang H, Zhang X. Identification of Metronidazole Tablets by Infrared Spectrophotometry. *China Pharmacy*, 2005, 16(8):619-620.
[45] Ge, M.; Xi, Z.; Zhu, C.; Liang, G.; Hu, G.; Jamal, L.; S. M., J. A. Preparation and Characterization of Magadiite–Magnetite Nanocomposite with Its Sorption Performance Analyses on Removal of Methylene Blue from Aqueous Solutions. Polymers 2019, 11 (4), 607.
[46] Mandapalli PK, Venuganti VVK. Layer-by-layer microcapsules for pH-controlled delivery of small molecules. *Journal of Pharmaceutical Investigation* **2015**, *45*, 131–141.
[47] Ding A, Zhou Y, Chen P, Nie W. Ibuprofen-loaded micelles based on star-shaped erythritol-core PLLA-PEG copolymer: effect of molecular weights of PEG. *Colloid Polym Sci* **2017**, *295*, 1609–1619.
[48] Ge M, Tang W, Du M, Liang G, Hu G, Jahangir Alam SM. Research on 5-fluorouracil as a drug carrier material with its in vitro release properties on organic modified magadiite. *European Journal of Pharmaceutical Sciences* **2019**,*130*, 44–53.
[49] Nhavene EPF, da Silva WM, Trivelato Junior RR, Gastelois PL, Venâncio T, Nascimento R, et al. Chitosan grafted into mesoporous silica nanoparticles as benznidazol carrier for Chagas diseases treatment **2018**, *272*, 265–275.
[50] Huanbutta K, Nernplod T, Akkaramongkolporn P, Sriamornsak P. Design of porous Eudragit® L beads for floating drug delivery by wax removal technique. *Asian Journal of Pharmaceutical Sciences* **2017**, *12*, 227–234.
[51] Mingliang G, Yueying L, Caiping Z, Guodong L, Jahangir A.S.M., Guoqing H, Yuee G, Junaebur R.M. Preparation of organic-modified magadiite–magnetic nanocomposite particles as an effective nanohybrid drug carrier material for cancer treatment and its properties of sustained release mechanism by Korsmeyer–Peppas kinetic model. *Journal of Materials Science* **2021**, 03 June 2021, 1-17.